

Electrochemical Synthesis of a Binary Mn-Co Oxides Decorated Graphene Nanocomposites for Application in Nonenzymatic H₂O₂ Sensing

*Su-Juan Li**, Yun Xing, Hong-Yuan Yang, Jia-Yan Huang, Wen-Tian Wang, Rui-Ting Liu

Henan Province Key Laboratory of New Optoelectronic Functional Materials, College of Chemistry and Chemical Engineering, Anyang Normal University, Anyang, 455000, Henan, China.

*E-mail: lemontree88@163.com

Received: 12 April 2017 / *Accepted:* 11 May 2017 / *Published:* 12 June 2017

In this work, binary metallic oxides of MnO₂-Co₃O₄ nanocomposite was electrodeposited on graphene oxide (GO) modified electrode by a facile and one-step electrochemical method. The resultant MnO₂-Co₃O₄/graphene (MnO₂-Co₃O₄/GP) electrode was characterized by scanning electron microscopy (SEM) and energy dispersive X-ray spectroscopy (EDX) to study its morphology and element composition. The as-prepared MnO₂-Co₃O₄/GP modified electrode was employed in fabricating a nonenzymatic H₂O₂ electrochemical sensor. The cyclic voltammetry (CV) and amperometric experiments demonstrated that the MnO₂-Co₃O₄/GP composites exhibited superior electrocatalytic activities toward oxidation of H₂O₂ to the monometallic oxide decorated graphene materials (MnO₂/GP and Co₃O₄/GP). The developed nonenzymatic H₂O₂ sensor showed a high sensitivity of 53.65 μA mM⁻¹ cm⁻², a wide linear range of 5 μM-1.2 mM, and a detection limit of 0.8 μM (S/N = 3). In addition, good selectivity, high detection accuracy and acceptable stability were also obtained for the present sensor. Therefore, this work will open an avenue to construct high-performance electrode materials and expand their applications in various fields such as catalysis and biosensor.

Keywords: Electrochemical; Graphene; binary metallic oxides; Hydrogen peroxide

1. INTRODUCTION

In recent years, growing research interest has been paid to the design and preparation of bimetallic or bimetallic oxides/hydroxides nanomaterials due to the fact that diverse properties and even better performance than their corresponding monometallic counterparts can be generated under the coordination effect of these two nanobuilding blocks. It was currently demonstrated that the

hybrids of Cu-Co alloy dendrites [1], Ni-Co nanostructures [2], Ni-Cu-oxide nanowire arrays [3] and NiO_x/MnO_x nanoparticles [4] exhibited superior performance to both their corresponding individual components toward oxidation of glucose or hydrogen peroxide (H₂O₂) in terms of excellent electrocatalytic activities and high detection sensitivity. The nanohybrid of Co₃O₄@MnO₂ [5] has been reported to display a significant increase (4-10 times) in areal capacitance compared to single Co₃O₄ nanomaterials. Ni_xCo_{2x}(OH)_{6x}/graphene hybrids [6] have been demonstrated to exhibit improved specific capacitance along with rate capability in comparison with those of Ni(OH)₂ or Co(OH)₂ materials on graphene support. In addition, for electrochemical biosensor application, the Ni_xCo_{2x}(OH)_{6x}/graphene nanohybrid electrode exhibits excellent performance towards the nonenzymatic detection of H₂O₂.

As important transition metal oxides materials, MnO₂ and Co₃O₄ have been extensively explored as electrochemical H₂O₂ sensors [7-13], driven by their distinct electrocatalytic activity to oxidation of H₂O₂, and the characteristic properties of these materials with high abundance, environmental friendly and low cost. However, MnO₂ suffers from poor electric conductivity (10⁻⁵–10⁻⁶ S cm⁻¹) [14,15], which limits its electron transfer capability and thus its electrochemical performance. Through integration of MnO₂ with higher conductive Co₃O₄, the improved electrical conductivity along with electrochemical activity is expected to demonstrate. Importantly, the attributes of MnO₂ and Co₃O₄ in this binary composites can be combined together to form highly efficient electrocatalyst. To further enhance the electric conductivity of this MnO₂-Co₃O₄-based electrochemical sensing material, the effective strategy is to introduction of various carbon materials like carbon foam [15], graphene or its derivatives [16-19], carbon nanotube [20-23] and ordered mesoporous carbon (OMC) [24] as support materials. Among these carbon materials, graphene (GP), with a single layer of sp² hybridized carbon atoms, has arisen widespread interest in electrochemical applications [25,26]. Accordingly, a binary Mn-Co oxides decorated graphene (MnO₂-Co₃O₄/GP) composite is expected to exhibit high electrocatalytic activities and shows prospects for application in fabricating highly efficient H₂O₂ sensors.

Inspired by the unique properties of MnO₂-Co₃O₄/GP composites, herein, a new type of a binary Mn-Co oxides decorated graphene nanocomposite was fabricated by a facile and green one-step electrochemical method and utilized directly as nonenzymatic sensors for H₂O₂ detection. The MnO₂-Co₃O₄/GP composite was firstly prepared by solution-casting of graphene oxide (GO) nanosheets on surface of glassy carbon electrode (GCE), followed by simultaneous electrochemical reduction of GO and electrodeposition of MnO₂-Co₃O₄ nanoparticles on it. To our best knowledge, it is the first successful attempt to synthesize MnO₂-Co₃O₄/GP composite by means of one-step electrochemical reduction method. The MnO₂-Co₃O₄/GP composite exhibited excellent electrocatalytic activities toward oxidation of H₂O₂, thus the resultant sensors presented low detection limit, high sensitivity, wide linear range and rapid response towards the detection of H₂O₂. Consequently, the proposed strategy for the fabrication of binary metal oxide/graphene composites in this work will provide new insights on designing facile and highly efficient electrode materials for various applications.

2. EXPERIMENTAL SECTION

2.1. Reagents and materials

GO was supplied by Nanjing XFNANO Materials Tech Co., Ltd. $\text{Mn}(\text{CH}_3\text{COO})_2 \cdot 4\text{H}_2\text{O}$, glucose, H_2O_2 , ascorbic acid (AA), dopamine (DA), uric acid (UA), L-tyrosine were obtained from Sinopharm Chemical Reagent Co., Ltd. (Shanghai, China) without the further purification. K_2HPO_4 and NaH_2PO_4 were used to prepare the supporting electrolyte of 0.1 M phosphate buffer solution (PBS, pH 7.0). Deionized water (18.2 M Ω cm) was prepared by a Milli-Q water purification system.

2.2. Apparatus

The surface morphology and the element component of synthesized modified electrode was characterized by field emission scanning electron microscopy with EDX equipped (FESEM, JSM-6701F, Japan). Electrochemical measurements were performed on a CHI 660D electrochemical analyzer (CHI Instruments Shanghai, China) with a conventional three-electrode system. The

$\text{MnO}_2\text{-Co}_3\text{O}_4/\text{GP}$ composite modified glassy carbon electrode ($\text{MnO}_2\text{-Co}_3\text{O}_4/\text{GP}/\text{GCE}$) was used as the working electrode, a saturated calomel electrode (SCE) as the reference electrode and a Pt wire as counter electrode.

2.3. Electrochemical preparation of $\text{MnO}_2\text{-Co}_3\text{O}_4/\text{GP}$ composite modified electrode

Prior to modification, a bare glassy carbon electrode (diameter of 3 mm) was carefully polished with 1.0, 0.3 and 0.05 μm alumina slurries respectively to obtain a mirror-like surface. The polished electrode was ultrasonicated in ethanol and deionized water in sequence. Then, 10 μL 1 mg/mL GO aqueous solution was coated onto electrode surface, and allowed to dry to obtain GO modified electrode (GO/GCE). The obtained GO/GCE was subsequently immersed into deposition solutions containing with 0.1 M Na_2SO_4 +5 mM CoCl_2 +5 mM $\text{Mn}(\text{CH}_3\text{COO})_2$, and cycled under the potential window from -1.5 V to 0 V for 10 cycles. Through this electrochemical process, GO was electrochemically reduced to GP, meanwhile, Mn-Co oxides was electrodeposited on GP surface to form $\text{MnO}_2\text{-Co}_3\text{O}_4/\text{GP}$ composites modified electrode ($\text{MnO}_2\text{-Co}_3\text{O}_4/\text{GP}/\text{GCE}$). For comparison, The electrodes modified with GP, and monometallic Co or Mn oxides decorated GP were separately prepared by immersing the GO/GCE into deposition solutions of 0.1 M Na_2SO_4 without (for GP/GCE) and with only 5 mM CoCl_2 (for $\text{Co}_3\text{O}_4/\text{GP}/\text{GCE}$) or 5 mM $\text{Mn}(\text{CH}_3\text{COO})_2$ (for $\text{MnO}_2/\text{GP}/\text{GCE}$) involved, respectively, according to the same electrochemical method described above.

2.4 Electrochemical sensing of H_2O_2

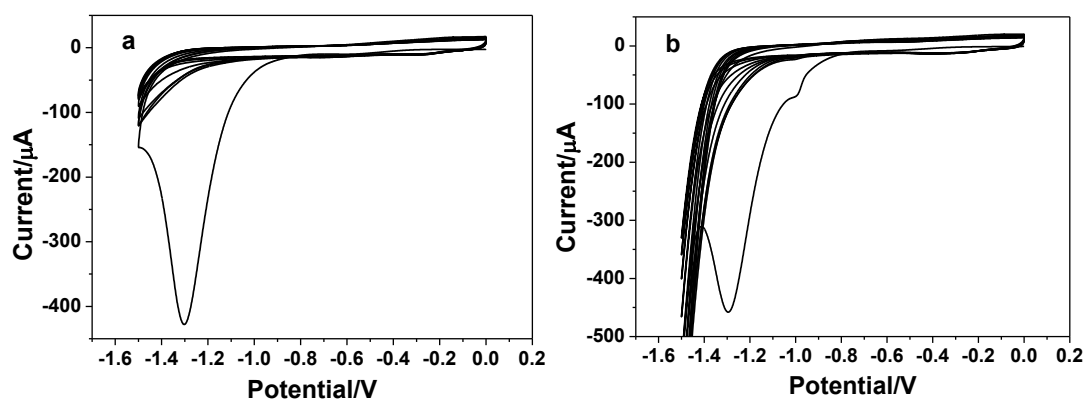
The electrochemical behavior of H_2O_2 was investigated by cyclic voltammetry (CV) technique in the potential range of -0.4~0.8 V. The amperometric sensing of H_2O_2 was performed at an applied potential of +0.5 V by adding various aliquots of H_2O_2 stock solution into electrochemical cell with 10

mL 0.1 M PBS (pH 7.0) contained. The PBS solution was kept continuously stirred to make the concentration of added H_2O_2 uniform. Current-time curve was performed to record the steady state current response with interval of 50 s for every addition of H_2O_2 .

3. RESULTS AND DISCUSSION

3.1. CV responses for the formation of the modified electrodes and the morphology characterization

Fig. 1 exhibits the CV responses for the formation processes of thus fabricated GP, $\text{Co}_3\text{O}_4/\text{GP}$, MnO_2/GP , and $\text{MnO}_2\text{-Co}_3\text{O}_4/\text{GP}$ modified electrode. As seen from Fig. 1a, at a scanning potential range from 0 to -1.5 V, the CVs of GO/GCE in solutions of 0.1 M Na_2SO_4 present a large cathodic peak current at around -1.3 V *vs.* SCE in the first cycle. In the subsequent cycles, the cathodic peak current significantly decreases and even disappears, which indicates that the surface-oxygenated groups of GO have been quickly reduced to form graphene. This phenomenon is consistent with previous results [27,28]. When the GO/GCE was immersed into 0.1 M Na_2SO_4 solution with 5 mM CoCl_2 involved, a new cathodic peak at -1.0 V corresponding to reduction of Co^{2+} was observed in the CVs of Fig. 1b, apart from the cathodic peak at -1.3 V related to GO reduction. In the presence of dissolved oxygen, the deposited Co was oxidized to Co_3O_4 . By using this CV method, the previous works also demonstrates the successful formation of Co_3O_4 on electrode surface [11,29-31]. Recently, the electrochemical method, such as CV or constant applied potentials, has also been widely used for electrodeposition of MnO_2 materials from precursor of Mn^{2+} [19,20,24]. Here, the CV method was used. As can be seen from Fig. 1c, another new cathodic peak at about -0.9 V corresponding to reduction of Mn^{2+} appeared in the CVs of GO/GCE with deposition solutions of 0.1 M Na_2SO_4 +5 mM $\text{Mn}(\text{Ac})_2$, apart from the cathodic peak at -1.3 V corresponding to GO reduction. The obtained CV curves are in good agreement with that of Dong's work in which the one-step electrochemical approach is developed for synthesis of graphene/ MnO_2 nanowall hybrids [32]. Therefore, the hybrids of MnO_2/GP are estimated to be formed on electrode surface. Interestingly, with the GO/GCE immersed into the deposition solutions of 0.1 M Na_2SO_4 +5 mM CoCl_2 +5 mM $\text{Mn}(\text{Ac})_2$, the obtained CV curves (Fig. 1d) integrate the feature of the respective CV curves of Fig. 1b and c.



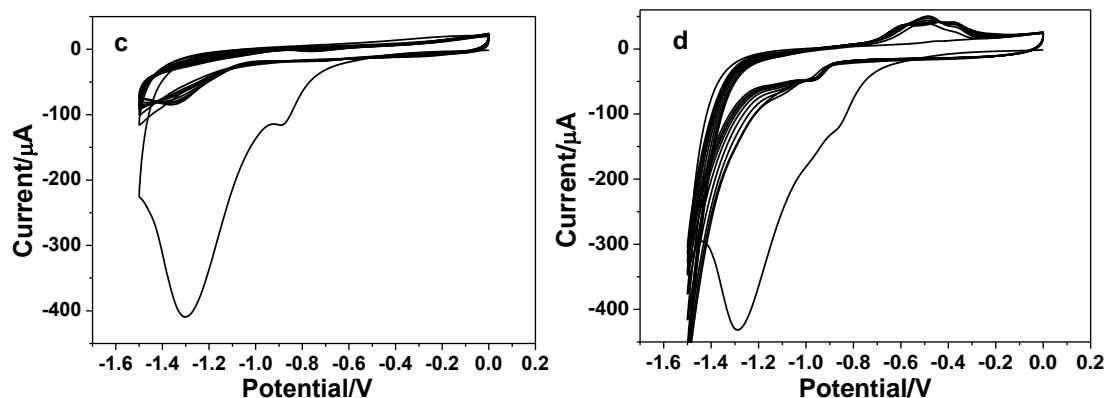


Figure 1. The CV responses of GO/GCE in deposition solutions of (a) 0.1 M Na_2SO_4 , (b) 0.1 M Na_2SO_4 +5 mM CoCl_2 , (c) 0.1 M Na_2SO_4 +5 mM $\text{Mn}(\text{Ac})_2$ and (d) 0.1 M Na_2SO_4 +5 mM CoCl_2 +5 mM $\text{Mn}(\text{Ac})_2$ for 10 cycles to prepare the GP/GCE, Co_3O_4 /GP/GCE, MnO_2 /GP/GCE and MnO_2 - Co_3O_4 /GP/GCE, respectively.

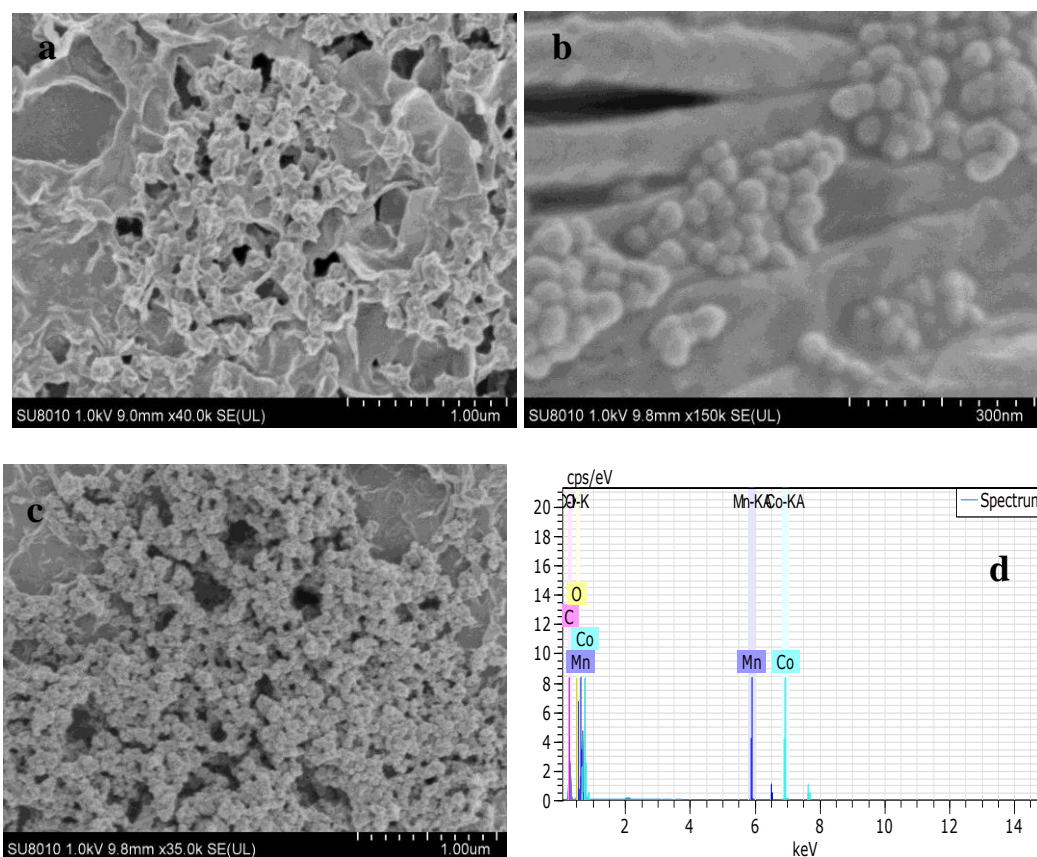


Figure 2. FESEM images of the prepared MnO_2 /GP/GCE (a), Co_3O_4 /GP/GCE (b), MnO_2 - Co_3O_4 /GP/GCE (c) and the EDX spectra of MnO_2 - Co_3O_4 /GP/GCE.

Three distinct cathodic peaks at -1.3 , -1.0 and -0.9 V correspond to the reduction of GO, Co^{2+} and Mn^{2+} , respectively, to obtain the resulting MnO_2 - Co_3O_4 /GP modified electrode. The above results suggest that the proposed one-step electrochemical method is feasible for preparation of binary Mn-Co oxides decorated graphene nanocomposites. The surface morphology of the prepared MnO_2 /GP/GCE,

$\text{Co}_3\text{O}_4/\text{GP}/\text{GCE}$, $\text{MnO}_2\text{-Co}_3\text{O}_4/\text{GP}/\text{GCE}$ was characterized by FESEM images, the results of which were displayed in Fig. 2.

As can be seen from Fig. 2a, the wrinkled surface of the RGO film is decorated with flower-like MnO_2 nanoparticles with diameters ranging from 50 to 100 nm. For $\text{Co}_3\text{O}_4/\text{GP}/\text{GCE}$ (Fig. 2b), about 20-30 nm Co_3O_4 nanoparticles were decorated onto RGO surface. However, for $\text{MnO}_2\text{-Co}_3\text{O}_4/\text{GP}/\text{GCE}$, more densely and aggregated nanoparticles with diameters of about several tens nanometer sized nanoparticles were electrodeposited onto RGO surface. From the EDX result presented in Fig. 2d, the elements of C, O, Mn and Co were all observed, indicating that the $\text{MnO}_2\text{-Co}_3\text{O}_4/\text{GP}$ nanocomposites have been successfully synthesized on electrode surface.

3.2. Electrochemical behavior of H_2O_2 at the Mn-Co oxides/GP nanocomposites modified electrode

In order to verify the electrocatalytic activity of the synthesized materials for H_2O_2 oxidation, the CV experiments toward H_2O_2 was performed. Fig. 3a shows CV responses of different modified electrodes in 5 mM H_2O_2 at pH 7.0 PBS solution. As observed, the oxidation of H_2O_2 starts from a potential of +0.4 V at the three electrodes of GP/GCE, $\text{MnO}_2/\text{GP}/\text{GCE}$ and $\text{Co}_3\text{O}_4/\text{GP}/\text{GCE}$, and the oxidation currents of H_2O_2 at $\text{MnO}_2/\text{GP}/\text{GCE}$ and $\text{Co}_3\text{O}_4/\text{GP}/\text{GCE}$ are obviously larger than that of GP/GCE, suggesting that the presence of MnO_2 and Co_3O_4 on GP surface play significant roles for electrocatalyzing the oxidation of H_2O_2 . Therefore, cobalt and manganese oxide nanoparticles are both appropriate as mediators to shuttle electron between sensing electrode and analyte of H_2O_2 . The similar results have been displayed in previous works [7-13]. However, at $\text{MnO}_2\text{-Co}_3\text{O}_4/\text{GP}/\text{GCE}$, the addition of H_2O_2 results in a significant current increase for oxidation of H_2O_2 with onset potential of +0.3 V, which is more negative than +0.4 V, meanwhile, the oxidation current increase prominently compared to the other three electrodes. These results demonstrate that the integration of MnO_2 and Co_3O_4 exhibits higher electrocatalytic activities toward oxidation of H_2O_2 , and the electron exchange between modified electrode and H_2O_2 is thus further facilitated. This phenomenon is mainly ascribed to the synergistic effects of the MnO_2 and Co_3O_4 materials resulting in excellent electrocatalytic activities toward oxidation of H_2O_2 . In addition, the good electrical conductivity of $\text{MnO}_2\text{-Co}_3\text{O}_4/\text{GP}$ nanocomposites also enhanced its electrochemical performance.

The priority of $\text{MnO}_2\text{-Co}_3\text{O}_4/\text{GP}$ nanocomposites modified electrode to electrodes modified with GP/GCE, $\text{MnO}_2/\text{GP}/\text{GCE}$ and $\text{Co}_3\text{O}_4/\text{GP}/\text{GCE}$ was further verified from amperometric results. Fig. 3b shows amperometric responses of various electrodes to successive additions of 100 μM H_2O_2 at an applied potential of +0.5 V. As observed, the current response of $\text{MnO}_2\text{-Co}_3\text{O}_4/\text{GP}/\text{GCE}$ toward H_2O_2 is obviously higher than the other three modified electrodes, which further indicates that the synergistic effects between binary metallic oxides and the enhanced electrical conductivity by the introduction of graphene.

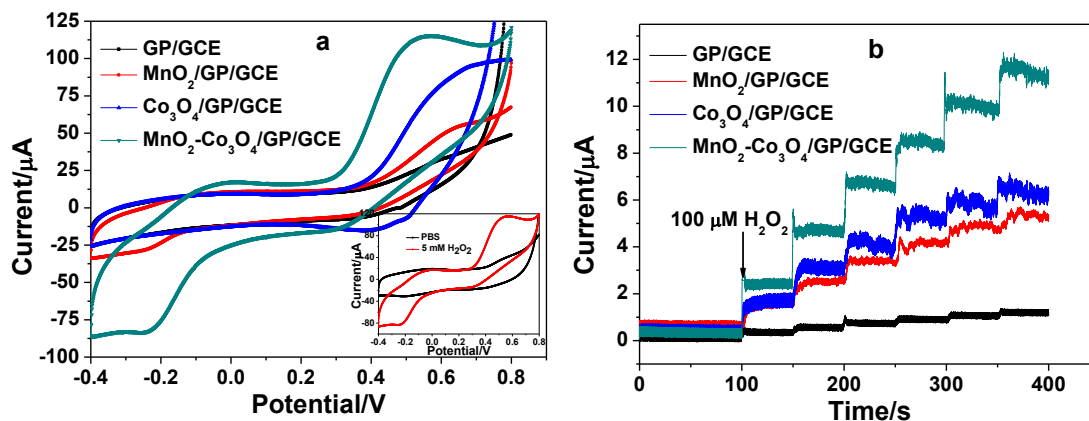


Figure 3. The CV (a) and the amperometric (b) responses of GP/GCE, MnO₂/GP/GCE, Co₃O₄/GP/GCE and MnO₂-Co₃O₄/GP/GCE. The CVs of MnO₂-Co₃O₄/GP/GCE in 0.1 M PBS (pH 7.0) in the absence and presence of 5 mM H₂O₂ is shown in the inset of Fig.3a.

3.3. Amperometric detection of hydrogen peroxide

Amperometric technique was utilized to evaluate the electrochemical performance of the MnO₂-Co₃O₄/GP/GCE for determination of H₂O₂. The typical amperometric responses of the MnO₂-Co₃O₄/GP/GCE were presented in Fig. 4a upon dropwise additions of H₂O₂ into pH 7.0 PBS to increasing concentrations with an applied potential of +0.5 V. Immediately after the addition of H₂O₂, the oxidation current of the sensor responded rapidly and reached 95% of the steady-state current within 3 s, showing a fast response time for amperometric detection of H₂O₂. The calibration curve displayed in Fig. 4b indicates that the oxidation currents increase linearly with the increase of the H₂O₂ concentration. The linear range spans the concentration range from 5 µM to 1.2 mM with the linear regression equation of $I (\mu\text{A}) = 0.30537 + 0.00379C (\mu\text{M})$ (correlation coefficient of 0.9972). The amperometric sensitivity of the sensor was calculated to be 53.65 µA mM⁻¹ cm⁻² and the limit of detection (LOD) was estimated to be 0.8 µM based on a signal-to-noise ratio of 3.

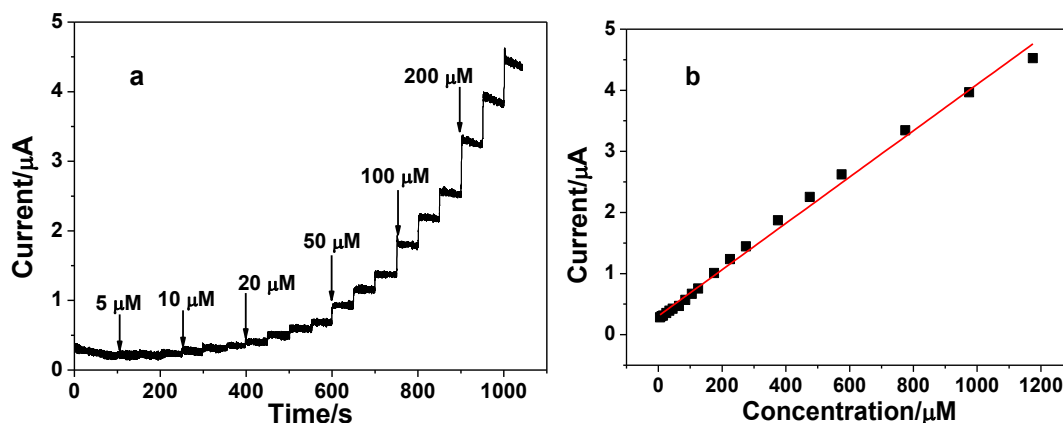


Figure 4. Amperometric responses of the MnO₂-Co₃O₄/GP/GCE (holding at +0.5 V) upon addition of H₂O₂ to increasing concentrations (a) and the corresponding calibration curve (b).

To assess the anti-interference ability of the $\text{MnO}_2\text{-Co}_3\text{O}_4/\text{GP}/\text{GCE}$, the effect of potential interfering species including glucose, L-tyrosine, DA, AA and UA was examined, as shown in Fig. 5. There is a significant oxidation current response for the addition of 1 mM H_2O_2 . In contrast, the current responses generated by addition of 1 mM glucose, L-tyrosine and UA can hardly be observed, and the current responses of 1 mM of DA and AA are also small. The amperometric response current ratios to H_2O_2 and the above interfering species on $\text{MnO}_2\text{-Co}_3\text{O}_4/\text{GP}/\text{GCE}$ were shown in Fig. 5b. There are no significant interferences observed upon addition of those interfering species into analyte of H_2O_2 , indicating a high selectivity for the present $\text{MnO}_2\text{-Co}_3\text{O}_4/\text{GP}$ composites based H_2O_2 sensor. In addition, the reproducibility of the prepared $\text{MnO}_2\text{-Co}_3\text{O}_4/\text{GP}/\text{GCE}$ was studied by preparing six electrodes separately under the same conditions. The oxidation current responses of these six electrodes toward 100 μM H_2O_2 yielded a relative standard deviation (RSD) of only 3.4%, which indicates an acceptable reproducibility. For one $\text{MnO}_2\text{-Co}_3\text{O}_4/\text{GP}/\text{GCE}$, it was stored in room temperature for 20 days and the current was periodically measured. It can be found that the current response retains 92% of its initial value after storage of 20 days. All of these results demonstrated that the prepared $\text{MnO}_2\text{-Co}_3\text{O}_4/\text{GP}/\text{GCE}$ displayed an excellent electrocatalytic activity, good selectivity and stability toward H_2O_2 detection.

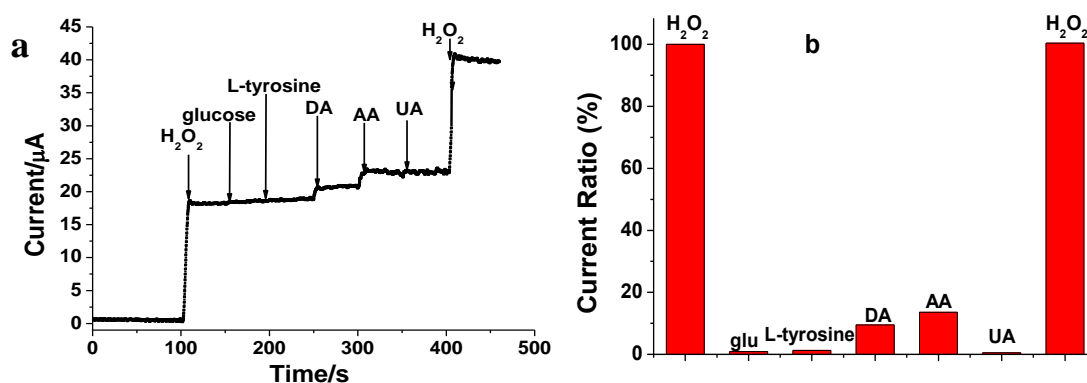


Figure 5. (a) Amperometric responses of the $\text{MnO}_2\text{-Co}_3\text{O}_4/\text{GP}/\text{GCE}$ to successive additions of 1 mM H_2O_2 , 1 mM DA, 1 mM H_2O_2 , 1 mM AA, 1 mM L-tyrosine and 1 mM UA; (b) Amperometric current response ratio of the above interfering species on that of H_2O_2 .

For comparison, the performance of our present $\text{MnO}_2\text{-Co}_3\text{O}_4/\text{GP}$ composites with various MnO_2 and Co_3O_4 based materials to H_2O_2 sensing is listed in Table 1. Obviously, compared to several H_2O_2 sensors reported previously [9,16,33], the present $\text{MnO}_2\text{-Co}_3\text{O}_4/\text{GP}$ composites possessed comparable and even better analytical parameters in terms of high detection sensitivity, appropriate linear range and low LOD, suggesting that the fabricated $\text{MnO}_2\text{-Co}_3\text{O}_4/\text{GP}$ composites modified electrode might serve as a highly efficient and promising enzyme-free H_2O_2 sensor. Furthermore, the applied oxidation potential (+0.5 V) for detection of H_2O_2 in this work is much more negative than some of other materials, for example, MnO_2 microspheres [9], $\text{MnO}_2/\text{carbon fiber}$ [33] and $\text{CoOxNPs}/\text{ERGO}$ [13], which potentially reduce the possible interference of oxidative substances coexisting with H_2O_2 . The good and acceptable performance of the present $\text{MnO}_2\text{-Co}_3\text{O}_4/\text{GP}$

composites could be attributed to the following reasons. First, the MnO₂-Co₃O₄ binary composites exhibit high electrocatalytic activities toward H₂O₂ oxidation arising from their synergistic effects, which significantly enhanced the detection performance. Second, the introduction of graphene improves the electrical conductivity of the resultant MnO₂-Co₃O₄/GP composites, which favors the electron transfer and thus guarantees the full utilization of MnO₂-Co₃O₄ binary composites. It is also point out that the proposed sensor is at the neutral biological conditions for detection of H₂O₂, which is different from other MnO₂ based sensors to carry out in strong alkaline media [16,21], thus, the present method has the potential prospect to direct and on-line analyze and determine H₂O₂ in biological samples.

Table 1 Comparison of MnO₂-Co₃O₄/GP composites with various MnO₂ and Co₃O₄ based materials to H₂O₂ sensing.

Electrode materials	Potential (V)	Sensitivity ($\mu\text{A mM}^{-1} \text{cm}^{-2}$)	Linear range	LOD (μM)	Ref.
MnO ₂ microspheres	+0.8	-	10 -150 μM	2	9
CoO _x NPs/ERGO	+0.75	148.6	5 μM -1 mM	0.2	13
MnO ₂ -carbon foam	-0.45 V	-	2.5 μM - 2.055 mM	0.12	15
MnO ₂ /GO	-0.3 V	38.2	5 μM -0.6 mM	0.8	16
MnO ₂ -ERGO	-0.5	59.0	0.1-45.4 mM	10	19
MnO ₂ /VACN Ts	+0.45 V	1080	1.2 μM -1.8 mM	0.8	20
MnO ₂ /OMC	+0.45	806.8	0.5 μM -0.6 mM	0.07	24
MnO ₂ /carbon fiber	+0.58V	0.75 $\mu\text{A mM}^{-1}$	12-260 μM	5.4	33
MnO ₂ -Co ₃ O ₄ /GP	+0.5	53.65	5 μM -1.2 mM	0.8	This work

3.4. Real sample analysis

In order to verify the applicability of the MnO₂-Co₃O₄/GP composites based sensor, the content of H₂O₂ in real hydrogen peroxide samples that was stored at room temperature for 3 years was determined by the present method. The real samples were diluted with 0.1 M pH 7.0 PBS solution before determination. Another classical KMnO₄ titration method was also employed as a comparison to evaluate the confidence of the present electrochemical method. The determination results are displayed in Table 2. Obviously, the two results obtained from the different two methods for each sample are in good agreement, indicating that the proposed MnO₂-Co₃O₄/GP composites based sensor could be used for accurately determination of the H₂O₂ sample.

Table 2. Determination of H₂O₂ in real samples by the present electrochemical method and the KMnO₄ titration method.

Sample no.	This method (mM)	RSD (%) ^a	KMnO ₄ titration method (mM)	RSD (%) ^a
1	2.816	3.6	2.904	3.2
2	3.588	2.8	3.492	4.5

^a Obtained from four successive measurements.

4. CONCLUSIONS

In summary, binary metallic oxides of MnO₂-Co₃O₄ were decorated on GP modified electrode through a facile and green one step electrodeposition method to form MnO₂-Co₃O₄/GP composites. MnO₂-Co₃O₄/GP electrode exhibited high electrocatalytic activity toward oxidation of H₂O₂, thus, a significant current response and low oxidation over-potential were obtained. Due to the synergistic effects of binary metallic oxides and the enhanced electrical conductivity by the introduction of graphene, MnO₂-Co₃O₄/GP electrode showed high performance towards the nonenzymatic determination of H₂O₂, including high detection sensitivity, good selectivity, high accuracy, and acceptable stability. In addition, the present electrochemical sensor can be successfully used for determination of H₂O₂ in real samples. Therefore, the proposed MnO₂-Co₃O₄/GP based sensor displayed excellent electrochemical response for H₂O₂ oxidation, demonstrating its potential application in routine analysis of H₂O₂.

ACKNOWLEDGEMENTS

This work was supported by the Grants from the National Natural Science Foundation of China (21105002), the fund project for Young Scholar sponsored by Henan province (14HASTIT012) and for Henan Key Technologies R&D Program (122102310516, 12B150002).

References

1. H. B. Noh, K. S. Lee, P. Chandra, M. S. Won and Y. B. Shim, *Electrochim. Acta*, 61 (2012) 36.
2. L. Wang, X. Lu, Y. Ye, L. Sun and Y. Song, *Electrochim. Acta*, 114 (2013) 484.
3. R. Ding, J. Liu, J. Jiang, J. Zhu and X. Huang, *Anal. Methods*, 4 (2012) 4003.
4. S. M. El-Refaei, M. M. Saleh and M. I. Awad, *J. Power Sources*, 223 (2013) 125.
5. J. P. Liu, J. Jiang, C. W. Cheng, H. X. Li, J. X. Zhang, H. Hong and H. J. Fan, *Adv. Mater.*, 23 (2011) 2076.
6. S. Dong, A. Q. Dao, B. Zheng, Z. Tan, C. Fu, H. Liu and F. Xiao, *Electrochim. Acta*, 152 (2015) 195.
7. C. Zhang, Y. Zhang, Z. Miao, M. Ma, X. Du, J. Lin, B. Han, S. Takahashi, J. Anzai and Q. Chen, *Sens. Actuators B Chem.*, 222 (2016) 663.
8. A. Wang, P. Zhang, Y. Li, J. Feng, W. Dong and X. Liu, *Microchim. Acta*, 175 (2011) 31.
9. L. Zhang, Z. Fang, Y. Ni and G. Zhao, *Int. J. Electrochem. Sci.*, 4 (2009) 407.
10. K. Schachl, H. Alemu, K. Kalcher, H. Moderegger, I. Svancara and K. Vytras, *Fresenius J. Anal. Chem.*, 362 (1998) 194.

11. A. Salimi, R. Hallaj, S. Soltanian and H. Mamkhezri, *Anal. Chim. Acta*, 594 (2007) 24.
12. J. Xu, J. Cai, J. Wang, L. Zhang, Y. Fan, N. Zhang, H. Zhou, D. Chen, Y. Zhong, H. Fan, H. Shao, J. Zhang and C. Cao, *Electrochem. Commun.*, 25 (2012) 119.
13. S. Li, J. Du, J. Zhang, M. Zhang and J. Chen, *Microchim. Acta*, 181 (2014) 631.
14. J. Lee and H. Hong, *J. Appl. Electrochem.*, 45 (2015) 1153.
15. S. He, B. Zhang, M. Liu and W. Chen, *RSC Adv.*, 4 (2014) 49315.
16. L. Li, Z. Du, S. Liu, Q. Hao, Y. Wang, Q. Li and T. Wang, *Talanta* 82 (2010) 1637.
17. M. R. Mahmoudian, Y. Alias, W. J. Basirun, P. M. Woi and M. Sookhakian, *Sens. Actuators B Chem.*, 201 (2014) 526.
18. Z. Wu, C. Li, J. Yu and X. Chen, *Sens. Actuators B Chem.*, 239 (2017) 544.
19. S. Dong, J. Xi, Y. Wu, H. Liu, C. Fu, H. Liu and F. Xiao, *Anal. Chim. Acta*, 853 (2015) 200.
20. B. Xu, M. Ye, Y. Yu and W. Zhang, *Anal. Chim. Acta*, 674 (2010) 20.
21. D. Ye, H. Li, G. Liang, J. Luo, X. Zhang, S. Zhang, H. Chen and J. Kong, *Electrochim. Acta*, 109 (2013) 195.
22. Y. Han, J. Zheng and S. Dong, *Electrochim. Acta*, 90 (2013) 35.
23. J. Chen, W. Zhang and J. Ye, *Electrochem. Commun.*, 10 (2008) 1268.
24. L. Luo, F. Li, L. Zhu, Z. Zhang, Y. Ding and D. Deng, *Electrochim. Acta*, 77 (2012) 179.
25. S. Li, C. Qian, K. Wang, B. Hua, F. Wang, Z. Sheng and X. Xia, *Sens. Actuators B Chem.*, 174 (2012) 441.
26. S. Li, D. Deng, H. Pang, L. Liu, Y. Xing and S. Liu, *J. Solid State Electrochem.*, 16 (2012) 2883.
27. H. L. Guo, X. F. Wang, Q. Y. Qian, F. B. Wang and X. H. Xia, *ACS Nano*, 3 (2009) 2653.
28. Z. Wang, X. Zhou, J. Zhang, F. Boey and H. Zhang, *J. Phys. Chem. C*, 113 (2009) 14071.
29. Z. Meng, B. Liu, J. Zheng, Q. Sheng, H. Zhang, *Microchim. Acta*, 175 (2011) 251.
30. A. Salimi, H. Mamkhezri, R. Hallaj, S. Soltanian, *Sens. Actuators B Chem.*, 129 (2008) 246.
31. S. Li, J. Du, J. Chen, N. Mao, M. Zhang, H. Pang, *J. Solid State Electrochem.*, 18 (2014) 1049.
32. C. Zhu, S. Guo, Y. Fang, L. Han, E. Wang and S. Dong, *Nano Res.*, 4 (2011) 648.
33. S. B. Hocevar, B. Ogorevc, K. Schachl and K. Kalcher, *Electroanalysis*, 16 (2004) 1711.

© 2017 The Authors. Published by ESG (www.electrochemsci.org). This article is an open access article distributed under the terms and conditions of the Creative Commons Attribution license (<http://creativecommons.org/licenses/by/4.0/>).